The Tale of Three Systems (ToTS) – Fate of Primary Production in the Chukchi Sea

Cruise report from *Sikuliaq* SKQ2023-10S

Kevin R. Arrigo, Chief Scientist
Stanford University

Introduction

Single-celled photosynthetic primary producers generate most of the fixed carbon (C) that ultimately supports Arctic Ocean food webs and drives numerous biogeochemical cycles. Three main sources of net primary production (NPP) have been identified in the Arctic Ocean that differ primarily in their timing and location within the water column but can also differ with respect to species composition and magnitude of NPP. These three NPP sources include (1) microalgae growing within the sea ice, (2) phytoplankton that bloom in water under the sea ice, and (3) phytoplankton that bloom in open water, including in the marginal ice zone (MIZ) and at the depth of the subsurface chlorophyll maximum (SCM). These blooms are part of what Stabeno et al. (2020) refer to as the Multiple Productive Layers of the Chukchi Sea (the MPL Hypothesis). There is growing evidence that the MPL hypothesis explains why the Chukchi Sea is so highly productive despite a short growing season. Moreover, the NPP and C export efficiency within these three bloom types likely controls the relative dominance by pelagic versus benthic ecosystems on shallow Arctic continental shelves, each of which supports unique assemblages of fish, birds, and mammals that humans rely on for food.

Because they are well adapted to growing at low light, the first of these three systems to bloom in the spring are the sea ice microalgae that can form dense assemblages at the bottom of the sea ice where access to seawater nutrients is greatest (Gradinger 2009). Composed primarily of pennate diatoms, these assemblages can reach chlorophyll *a* (Chl *a*) concentrations of >300 mg Chl *a* m^{-2} within the sea ice matrix (Arrigo 2017), sufficient to diminish light transmission through the ice and prevent phytoplankton growth in the water column below. Diatoms attached to ice crystal surfaces continue to grow until sea ice begins to melt in the spring. At that point, the ice algae slough off the bottom of the ice and sink through the water column, with much of the organic matter eventually reaching the seafloor (Cooper et al. 2005, Gradinger 2009). As such, sea ice ecosystems are a critical food source for benthic ecosystems in shallow Arctic seas and represent the only food for zooplankton prior to the spring phytoplankton bloom.

As spring progresses, light transmission through the ice and into the upper water column increases due to the loss of sea ice algae, the initiation of snow melt, and the formation of leads and melt ponds, allowing phytoplankton to bloom. The abundance of phytoplankton, primarily centric diatoms, within these under-ice blooms (UIBs) can reach extraordinary levels Arrigo et al. 2012, 2014). The fate of this massive production is still unknown, but because these UIBs form in cold waters early in the season, it is hypothesized that grazing losses are small and like sea ice algae, much of the biomass eventually reaches the sea floor on shallow Arctic shelves.

Once the sea ice retreats, the UIB may transition into an open water phytoplankton bloom or a new bloom may develop within the MIZ. This MIZ bloom tends to form in warmer, salinity stratified surface waters and the diatoms that dominate there consume most of the remaining nitrate (NO_3^-). Over the season, a SCM develops as the zone of maximum phytoplankton biomass descends to a depth where both NO_3^- and light are sufficient for net growth. Open water blooms are the best understood sources of NPP in the Arctic Ocean because they are easily sampled without entering the sea ice zone and are visible at large scales using satellites (Arrigo & Van Dijken 2015). However, it remains unclear whether the organic matter produced in these blooms is mostly grazed by zooplankton or sinks to the seafloor where it sustains the benthos.

Although all three of these blooms share the common attribute of being dominated by diatoms, the relative magnitude of NPP in these three systems is incompletely understood, as is the fate of the newly fixed C attributable to each. The particulate organic C (POC) produced in these three successive microalgal blooms supports both the pelagic and benthic ecosystems on shallow Arctic shelves. However, we do not yet know how the POC from these blooms is differentially partitioned between those pelagic and benthic ecosystems.

Another critical unknown is the relative importance of buoyancy regulation by microalgae in these three blooms in controlling their rate of descent within the water column. Vertical descent rate determines the proportion of POC that is remineralized within the water column, grazed during descent, or reaches the seafloor intact (Falkowski et al. 1998). It has been suggested that microalgal sinking speed is second only to growth rate as a key ecophysiological parameter controlling their importance to biogeochemistry and trophic interactions (Bannon & Campbell 2017). Thus, it is imperative that details of buoyancy regulation by sea ice microalgae, UIBs, and open water phytoplankton be characterized and compared to better understand their controls.

To date, progress in the area of buoyancy regulation has been hindered by our inability to characterize the sinking dynamics of individual particles that make up the exported POC flux. This problem has been solved by our development of a state-of-the-art imaging system (the Gravity Machine) that allows us to track individual particles and ensembles of particles, over several hours during their descent (Krishnamurthy et al. 2020). Early results from the Gravity Machine show that diatom cells exhibit an extraordinary ability to regulate their buoyancy over very short timescales (seconds) and can dramatically alter their rate of descent. Using the Gravity Machine, we can characterize the sinking dynamics of both sea ice algae and phytoplankton in unprecedented detail and quantify how sinking speeds vary as a function of taxa, physiological state, and environmental conditions such as temperature, light, and nutrient concentration. This new tool will be transformative to the study of export production in that it will provide for the first time, particle-level insight into the factors that control the relative organic matter export rates for the three dominant NPP sources in the Arctic Ocean.

Increasing our knowledge of the relative rates of NPP and particle export efficiency from these three systems is critical if we are to understand how continued sea ice loss, and the associated shifts in ice algal and phytoplankton bloom dynamics, will differentially impact benthic and pelagic food webs in shallow seas throughout the Arctic Ocean, including many organisms on which native human populations rely. Thus, the primary objectives of this proposed study are to utilize data obtained from a ship-based field program to the Chukchi Sea to 1) measure rates of NPP associated with the sea ice, UIBs, and open water phytoplankton in both the MIZ and SCM, 2) use sediment traps to characterize and quantify the vertical sinking fluxes of bulk particulate matter from the sea ice, UIBs, and open water phytoplankton blooms, and 3) use our Gravity Machine to determine how sinking speeds of microalgae from all three NPP sources vary by community composition, physiological state, and environmental conditions.

Overview of Study

The cruise took place from 16 June to 30 July 2023, beginning and ending in Nome, AK. Sampling was focused on two approximately parallel hydrographic sections that extended from open water to the south into the heavy pack ice to the north (Fig. 1). The Hanna Ridge (HR) transect was 123 km in length and the Hanna Ridge East (HRE) transect was 135 km in length. A segment of the Chukchi North (CN) line (46.5 km) connects the two transects. During the cruise, we did 7.5 counterclockwise circuits (387 km) along these lines (Fig. 1), resulting in eight HR sections, seven HRE sections, and seven short CH sections. Approximately half of our stations were conducted in the sea ice zone and half were in open water.

At 252 hydrographic survey stations within our main study region (Fig. 2), we measured vertical profiles of temperature, salinity, currents, light, and Chl *a* concentration. At a subset of these, we also collected samples to measure algal and microzooplankton abundance/species/size (PlanktoScope, n=200), algal physiology using the fast repetition rate fluorometer (FRRf, n=350), NPP (once per day), POC (n=400), particle sinking speeds (Hydrodynamic treadmill), deployed a Multi Corer to measure sediment Chl *a* (n=80), and deployed sediment traps to measure vertical fluxes of ice algae, phytoplankton, detritus, and fecal pellets (27). During transits, we continuously measured atmospheric conditions as well as sea surface temperature, salinity, nitrate, oxygen, pCO_2, and Chl *a* fluorescence from the various ship's systems to provide detailed maps of these parameters above and below the ice.

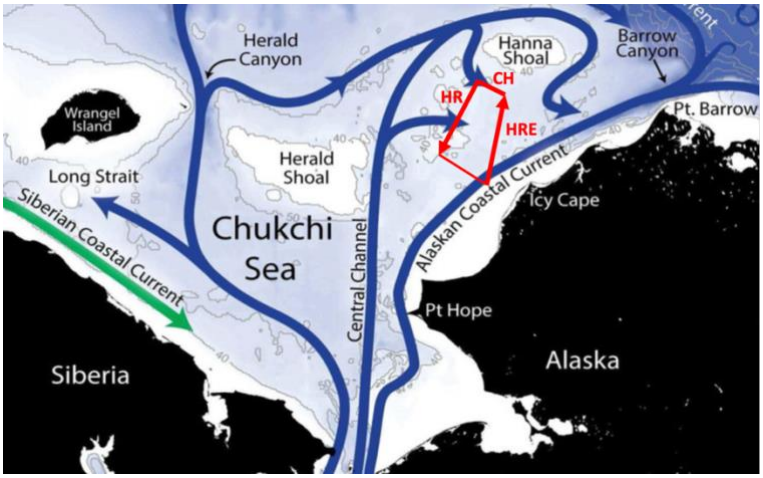

Figure 1. Location of the primary study region within the Chukchi Sea.

In the early stages of the cruise when the sea ice was safe to sample, we conducted 12 sea ice stations where we obtained ice cores to measure the temperature, salinity, and POC and Chl *a* concentration within the ice pack. We also deployed sediment traps through holes in the ice to measure sinking fluxes of algae, detritus, and fecal pellets from the sea ice and from the UIB.

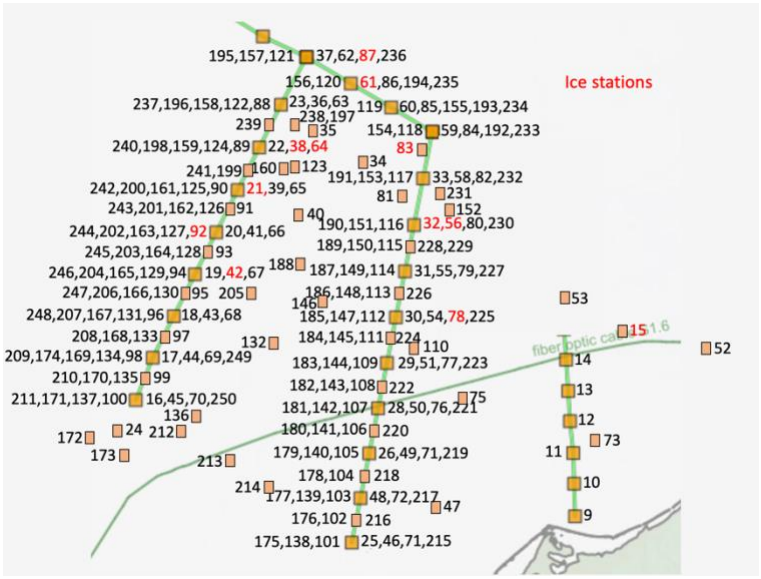

Figure 2. Station location within the primary study region within the Chukchi Sea. Ice stations are in red.

The ship was used as a platform for characterizing buoyancy regulation and measuring sinking speeds of microalgal cells and aggregates under various manipulated environmental conditions using the Gravity Machine. We also conducted experimental manipulations in four on-deck incubators to assess the phytoplankton sensitivity to UV radiation and measure transcripts of RNA as possible markers for nitrogen limitation.

Shipboard measurements

At each station, we deployed *Sikuliaq's* conductivity-temperature-depth (CTD) package, which consists of a Seabird 911+ with dual T/C sensors mounted on a rosette with 24 12-liter

Niskin bottles. The sensor suite also includes a Seabird SBE 43 dissolved O_2 probe, Biospherical QSP-2300 PAR sensor, Wetlabs C-Star transmissometer SN1609, WetLabs FLNTURTD chlorophyll fluorometer, and a Tritech PA 200/20 altimeter. Hull-mounted ADCP data were obtained throughout the cruise using *Sikuliaq's* 300 KHz instrument. Meteorological data were collected continuously using *Sikuliaq's* suite of anemometers.

Niskin bottles were used to collect seawater samples at 4-6 depths (e.g., 2, 10, 25, 50 m) and the SCM. Seawater at each depth was frozen and will be analyzed after the cruise for dissolved inorganic nutrients (NO_3^-, NO_2^-, PO_4^{3-}, and $Si(OH)_4$). Separate seawater samples were filtered for particulates (fluorometric Chl *a*, POC, and PON). For analysis of Chl *a*, seawater was filtered onto 25 mm Whatman glass fiber filters (GF/F, 0.7 µm nominal pore size) and extracted in the dark in 5 mL of 90% acetone for 24 hrs at 3°C prior to measurement (Holm-Hansen et al. 1965) on a Turner Designs 10-AU fluorometer calibrated with pure Chl *a* (Sigma-Aldrich). POC and PON will be analyzed after the cruise as described in Arrigo et al. (2017). Microalgal size structure and detailed taxonomic information at each station were quantified using an imaging PlanktoScope (www.planktoscope.org).

At each station, sinking characteristics of microalgae from either the sea ice, UIBs, the MIZ, or the SCM were assessed using our Gravity machine. Live microalgae collected fresh from each bloom type (at two depths for pelagic blooms, including the surface, SCM, and below the mixed layer) were introduced into the instrument and sinking characteristics of 10-12 individual cells and cell aggregates were monitored over 2–5-minute intervals. Sinking speeds were routinely measured under in situ conditions (within normal range of variability) and under different temperatures (-1 and 10°C) and NO_3^- concentrations (ambient and ambient + 5 µmol L^{-1}).

Each day, rates of water column NPP were measured using 24 hr simulated in situ deck incubations as described in Brown et al. (2015). To assess algal photophysiological state, we collected samples from two depths (2 and ~25 m or SCM) and assayed for differences in photosynthesis versus irradiance characteristics using FRRf, which provided estimates of maximum photosystem II (PSII) photochemical efficiency (Fv:Fm), effective cross-sectional area of PSII (σ), electron turnover time (τ) of PSII, and non-photochemical quenching (NPQ).

Samples for surface sediment Chl *a* measurements were obtained at 80 stations using a MC-800 Multi Corer (Ocean Instruments) and analyzed as described in Cooper et al. (2009).

Sea ice stations

In addition to the analyses described above, we also conducted on-ice surveys to measure snow depth, sea ice thickness, and collect sea ice cores. Ice cores were taken to determine vertical profiles of temperature, salinity, nutrient concentration, brine volume, Chl *a* concentration, microalgal species composition, and microalgal size structure. We deployed two sediment traps (one at 1 m and one at ~30 m) at each station to measure particle flux from the ice and from the UIB.

Ice cores for microbial characterization and enumeration were sectioned at 0.1 m intervals and segments placed in labeled polyethylene bags (Selz et al. 2018). All samples were stored in a dark thermally insulated cooler until processing on board ship (within 0.5 hr). Each section was then melted after adding 200 ml of 0.2 µm-filtered seawater to maintain salinity >28 (to minimize osmotic shock to the microbial assemblage). Meltwater from each sample was analyzed for fluorometric Chl *a* while assemblage composition was determined for the bottom 10 cm of each ice core only using the PlanktoScope. Cells from undiluted sea ice bottom (2-3 cm) samples were used to measure particle sinking speeds.

Sediment trap deployments

The sinking export of particulate material were measured at 27 (Fig. 3) stations using short-term free-drifting and ice-tethered particle interceptor traps, following methods used previously in Arctic and sub-Arctic seas (Juul-Pedersen et al. 2008, 2010, Pommier et al. 2009, Sallon et al. 2011, Lapoussière et al. 2013). Traps were deployed for 4-6 days at stations where hydrographic (Fig. 4) and biogeochemical measurements, including NPP, were made. At open water stations, free-drifting traps were deployed just below the euphotic zone (1% light depth), as recommended by Buesseler and Boyd (2009), and at approximately 30 m (the water column depth was ~40-50 m).

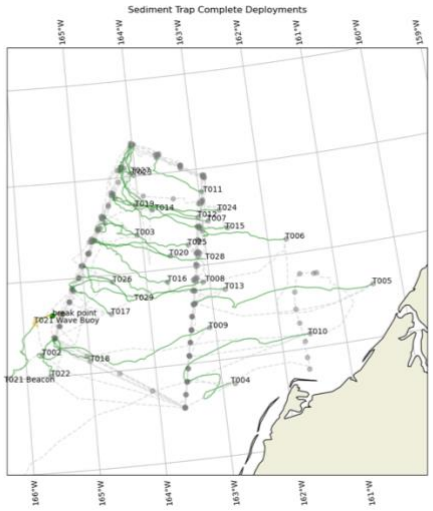

Figure 3. Trajectories of the 27 sediment traps deployed during this study.

The traps consist of PVC cylinders with an internal diameter of 10 cm and an aspect ratio (height:diameter) of 7:1. They were either ice-tethered using a wooden frame for support or deployed as free-drifting arrays. Iridium transmitters were used to track trap location. Prior to deployment, the traps were filled with artificial seawater at a salinity of 40-45. Trap deployments and handling were performed using JGOFS protocols (Knap et al. 1996) following the recommendations of Gardner (2000). The free-drifting trap arrays were surface-tethered with a series of small floats to minimize vertical motion on the trap line. Upon recovery, the collected material was sieved through a 450 µm mesh to remove potential large swimmers and processed for further analyses.

To minimize disturbance of the collected material, samples for microscopic examination and

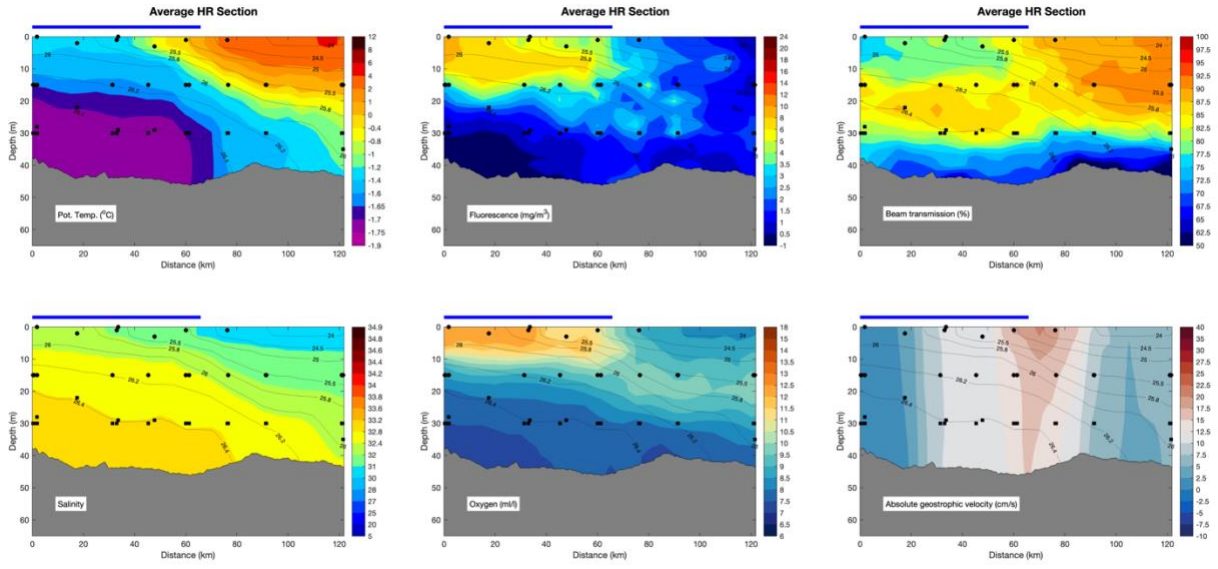

Figure 4. Hydrographic conditions at the location of sediment trap (black circles) releases along the Hanna Ridge transect.

density quantification (using the Gravity Machine) were taken first. Identification and enumeration of phytoplankton and other protists were conducted using the PlanktoScope. Chl *a*

and phaeopigments were measured fluorometrically as described above. Total particulate C, POC and PON will be measured on subsamples that were filtered onto pre-combusted (450°C for 24 h) Whatman GF/F filters.

Shipboard Acoustic Doppler Current Profiler Data Collection

Frank Bahr and Robert Pickart, Woods Hole Oceanographic Institution

Shipboard Acoustic Doppler Current Profiler (S-ADCP) data were collected throughout the cruise, primarily using *Sikuliaq's* high frequency WH300 given the shallow waters in the study area. Prior to the cruise, the WH300 had been replaced with a loaner from the University of Alaska, Fairbanks (UAF). Overall, the WH300 performed well, collecting over 10,000 five-minute profiles with 2 m vertical resolution. The onboard UHDAS acquisition software, developed and maintained by the ADCP group at the University of Hawaii (UH) (https://currents.soest.hawaii.edu) provided initial processing. Since performance is closely watched at UH via daily emails, this initial dataset tends to be of high quality. The reduced size of its 5-minute averages, compared to the voluminous single ping raw data, made it possible to transfer the data ashore as daily .zip files for further processing, thanks to the shoreside support provided by J. Haverlack (UAF) and *Sikuliaq's* marine technicians E. Shimada and B. McKiernan.

Frank Bahr met *Sikuliaq* in Nome prior to the cruise to assist in the setup of ADCP configurations and data transfer. During the cruise, he downloaded the .zip files and applied additional processing, including small calibration adjustments and visual editing. Occasional glitches around station arrival/departure as well as some remaining "fake" data from depths below the ocean floor were the main editing concerns. The calibration adjustments addressed two issues. The first consisted of a small alignment correction after the failure of the inflatable bladder system designed to ensure consistent alignment of the centerboard, which holds the WH300 as well as other instrumentation. The centerboard was lowered in ice-free conditions to drop the sensors below a bubble layer close to the ship but had to be retracted when breaking ice. Fortunately, the alignment changes following the bladder failure were small (a couple tenths of a degree at most).

A small adjustment was also applied to the overall ADCP scale factor, or "amplitude". Bottom track calibration amplitudes have been somewhat discredited in the past; however, they were confirmed here by a growing body of water track calibrations which compared the ADCP and GPS records of the ship's accelerations primarily from around CTD stations. Consequently, a 1.3% correction (amp factor 0.987) was applied that helped remove small differences between underway and on-station profiles. (For reference, the magnitude of this correction is similar to that of a 0.75-degree transducer rotation.)

Lastly, the OTPS tidal model version 3 (https://www.tpxo.net/otps) was used to estimate and remove the barotropic tide from the ADCP profiles. Tidal velocities were small (<5 cm s^{-1} in the main study area). Subsets of the final data from individual CTD sections were then plotted and saved into Matlab .mat files and emailed back to the ship to be combined with the hydrographic data to compute absolute geostrophic velocities.

Tater-ToTS

Matthew Mills, Stanford University
Jo Kaya, Moss Landing Marine Laboratories

Confirming the environmental controls on phytoplankton growth typically requires laborious incubations at sea that are time consuming to conduct and analyze. Results are often obtained weeks to months after the incubations are conducted. Furthermore, the laborious nature of shipboard incubations limits the spatial resolution at which controls on phytoplankton processes can be determined, and thus the spatial variability observed in many physical (e.g., temperature), chemical (e.g., nutrients, and biological (e.g., chlorophyll *a*) ocean parameters is missed when measuring the environmental controls on phytoplankton productivity. Analysis of phytoplankton RNA transcripts, the RNA strand produced when a gene is transcribed, may present a relatively fast way to assess the controls on phytoplankton growth at the same spatial scale as the environmental parameters. During the cruise, we conducted a total of eight experiments aimed at understanding if RNA transcripts involved in nutrient utilization (specifically nitrate) can be used as a diagnostic of N limitation of different phytoplankton taxa (e.g., diatoms and dinoflagellates).

Seawater was collected at a variety of stations that covered different environmental conditions (e.g., open water vs. ice covered waters, N replete vs. deplete). At each site, water was collected from one depth (surface or chlorophyll *a* maximum) into acid cleaned 2 L bottles. Bottles were left untreated and amended with either 5 µmol L^{-1} NO_3^-, or 5 µmol L^{-1} NH_4^+ and placed in a surface seawater flushed on-deck incubator that was covered with neutral density mesh that reduced incident irradiance by 50%. Bottles were sampled at t=48 and 72 hrs for nutrient (NO_3^-, NH_4^+, PO_4^{3-}, dSi), chlorophyll *a*, and particulate organic carbon concentrations. Additionally, samples were collected at each time point for determining photosynthetic parameters (e.g., efficiency of photosystem II (Fv:Fm) and the functional absorption cross section of photosystem II (σ_{PSII})) and the relative concentration of different phytoplankton taxa. Furthermore, we determined rates of CO_2fixation, as well as NO_3^- and NH_4^+ uptake. Lastly, water was collected onto 0.45 µm Supor (Sigma-Aldrich) membrane filters and preserved with RNAlater (Sigma-Aldrich) for eventual RNA extraction and transcript measurements.

In addition to the nutrient addition bottle assays, water was sampled daily along the cruise track for the analysis of transcript abundances. Water was collected from two depths (typically the surface and the chlorophyll *a* maximum) onto 10 µm nylon mesh filters and then preserved in RNAlater. In future analyses, we will extract and measure phytoplankton RNA transcripts related to nutrient and light utilization and then relate this to the along track distribution of nutrients and light conditions.

UV Experiments
Claudette Proctor, Stanford University

In order to test the hypothesis that sea ice shelters phytoplankton from harmful UV radiation and allows for the formation of under-ice blooms, we carried out a series of on deck incubation experiments. Water was collected from 12 stations (4 in ice, 8 in open water) in UV-transparent Whirlpak bags and incubated for 96 hours. To screen out UV radiation and simulate under-ice conditions, we used Acrylite OP-3 plexiglass. Various photosynthetically available radiation (PAR) levels were also simulated, using mesh neutral density screening bags. In total, there were six treatments, each one with one of two UV treatments (UV or No UV) and one of three PAR treatments (Low, Medium, or High). Measurements of chlorophyll, nutrients, and photosynthetic parameters were done at the initial, halfway, and final time points. Additional measurements at only the initial and final time points include particulate organic carbon (POC), light absorbance, and evaluation of community composition using the Planktoscope.

Gravity Machine and Planktoscope

Pranav Vyas, Grace Zhong, Qing Zhang, Stephanie Lim, Ethan Li

Gravity Machines

Most estimates to date of vertical carbon flux rely on bulk community approaches, such as sediment traps and oxygen/argon measurements. On our cruise, we used a scale-free vertical tracking microscopy (Hydrodynamic Treadmill or Gravity Machine) approach described in Krishnamurthy et al. (2020) to investigate sinking rates of diatoms. Briefly, 0.75 µm beads were added to concentrated seawater samples to enable Particle Image Velocimetry (PIV) in downstream analyses. Then, the samples were loaded into the Gravity Machine, a circular fluidic chamber with a rotational axis and a horizontally positioned microscope with two-axis tracking Individual particles were tracked using the 10X objective lens and convolutional neural network-based tracking. The resulting data include images of the tracked particle (5 fps) and x,y,z coordinates over a 2-minute period. These trajectories can then be used to quantify velocities.

We characterized the hydrodynamic behavior of various diatom species from three representative environments—sea ice, under-ice bloom, and open water—using the hydrodynamic treadmill. In particular, we analyzed 188 seawater samples from the CTD from the under-ice bloom and open water and 15 samples from melted ice cores at standard conditions of 0°C in the controlled temperature chamber. CTD seawater samples were taken from both the surface (2 m) and the subsurface chlorophyll maximum and concentrated on a 15 µm sieve after pre-filtration through 500 µm Nitex mesh. For each sample, we aimed to collect 20 tracks of different cells or groups of cells. Cells tracked were usually diatoms, singular or chained, and included species of *Fragilariopsis, Pseudo-nitzchia, Nitzchia, Chaetoceros, Thalassiosira,*, and *Navicula*. Other phytoplankton, including colonies of *Phaeocystis* were also tracked.

In addition, we conducted experiments to isolate the effects of temperature and nutrient conditions on sinking speeds. We conducted four temperature experiments in which we tracked samples from the same source water under two different controlled temperatures, 0°C and 10°C. This translated to estimate water temperatures of 0.5-2°C and 8-9°C, respectively. We conducted four nutrient experiments in which source waters were first incubated in on-deck incubators with flow-through seawater (shaded at 50% incident light) either unamended or with an 11 µmol L^{-1} NO_3^- addition. Samples were tracked after 24, 48, and/or 72 hour incubations. These experiments will complement the CTD and ice core samples to illuminate how environmental conditions may affect algal sinking speeds and behaviors.

Post-cruise processing will perform quality control on recorded tracks, calculate sinking rates, perform Particle Image Velocimetry, and analyze cells' hydrodynamic behaviors.

PlanktoScope

We used the PlanktoScope (Pollino et al. 2022), a new low-cost flow-imaging microscope, to quantify the microplankton community composition of various discrete-volume samples collected during this cruise.

To summarize, the PlanktoScope consists of a peristaltic pump connected downstream of a rectangular capillary flow cell, the contents of which are imaged by a Raspberry Pi (https://www.raspberrypi.com/) with a Raspberry Pi camera in a simple optical train consisting of a tube lens and an objective lens. The peristaltic pump operates in a stop-flow imaging sequence, in which a constant-volume unit of sample is pumped through the flow cell from a

sample input tube, an image is saved of the contents of the flow cell, and then another unit of sample is pumped through the flow cell, another image is saved, and so on. The acquired images of the flow cell are saved for subsequent processing to isolate cell images of individual objects, mostly consisting of phytoplankton, which can in turn be processed to calculate morphological and taxonomic metrics about the source sample.

On our cruise, the PlanktoScope was operated to complement the Imaging FlowCytobot (IFCB), which was exclusively in flow-through mode from continuous underway water throughout the cruise. In contrast, the PlanktoScope was used to analyze the 20 µm - 200 µm fraction of discrete-volume samples from Niskin bottles collected in CTD casts, from melted ice cores, from sediment traps, and from incubation experiments (simulated in situ production, TaTER-ToTS, and UV experiments).

We analyzed 292 seawater samples from 137 CTD stations (typically with samples collected from the surface and from the subsurface chlorophyll maximum), 12 samples from melted ice cores (collected from 11 stations), 48 samples from sediment traps (from 24 deployments of sediment traps at two depths per deployment), and 446 samples from incubation experiments. Our standard protocol for processing CTD samples was to concentrate each 500 mL sample by a factor of approx. 30-60 using a submerged 20 um filter, resulting in a concentrated suspended sample with a volume of approx. 8-15 mL; then to pass the >20 µm fraction of suspended sample through a 200 µm filter; and then to wash the 200 um filter with the <20 µm fraction of suspended sample, resulting in a final sample volume of approx. 12-20 mL depending on the visually-apparent biomass density in the sample. The concentration and dilution factors for each sample were recorded to enable quantitative comparison of absolute plankton counts across samples. The final samples were loaded into the PlanktoScope, which was configured to perform 400 stop-flow steps for each sample with a pumped volume of 0.02 mL per stop-flow step, resulting in 0.83 mL of sample imaged across a total of 400 raw images from 8 mL of each sample. Typically, the raw image datasets acquired from low-biomass samples contained approx. 100 - 500 individual objects in the >20 µm fraction (estimated from the PlanktoScope's official software algorithm to isolate individual objects from raw images), while datasets from high-biomass samples usually contained approx. 1500-6000 individual objects in the >20 um fraction.

For samples from melted ice cores and sediment traps, we used the same protocol but skipped the sample concentration steps; for samples from incubation experiments, we received sample which was pre-concentrated with a submerged 20 µm filter from either 250 mL or 500 mL (depending on the experiment) down to approx. 12-15 mL, which we then processed in the same way as the samples from melted ice cores and sediment traps.

Post-cruise processing will perform manual quality control on the saved raw images, more rigorous software-automated isolation of individual objects from the saved raw images, and calculation of various metrics from isolated objects to quantify each sample.

References

Arrigo, KR (2017) Sea ice as a habitat for primary producers. In: DN Thomas (Ed.) Sea Ice, Third Edition. John Wiley and Sons, Ltd.

Arrigo, KR, GL van Dijken (2011) Secular trends in Arctic Ocean net primary production. J Geophys Res 116, C09011, doi:10.1029/2011JC007151.

Arrigo, KR, GL van Dijken (2015) Continued increases in Arctic Ocean primary production. Prog Oceanogr 136, 60-70.

Arrigo, KR, DK Perovich, RS Pickart, ZW Brown, GL van Dijken, KE Lowry, MM Mills, MA Palmer, WM Balch, F Bahr, NR Bates, C Benitez-Nelson, B Bowler, E Brownlee, JK Ehn, KE Frey, R Garley, SR Laney, L Lubelczyk, J Mathis, A Matsuoka, BG Mitchell, GWK Moore, E Ortega-Retuerta, S Pal, CM Polashenski, RA Reynolds, B Scheiber, HM Sosik, M Stephens, JH Swift (2012) Massive phytoplankton blooms under Arctic sea ice. Science 336, 1408.

Arrigo, KR, DK Perovich, RS Pickart, ZW Brown, GL van Dijken, KE Lowry, MM Mills, MA Palmer, WM Balch, NR Bates, CR Benitez-Nelson, E Brownlee, KE Frey, SR Laney, J Mathis, A Matsuoka, BG Mitchell, GWK Moore, RA Reynolds, HM Sosik, JH Swift (2014) Phytoplankton blooms beneath the sea ice in the Chukchi Sea, Deep-Sea Res Part II 105, 1-16, http://dx.doi.org/10.1016/j.dsr2.2014.03.018.

Arrigo, KR, MM Mills, GL van Dijken, KE Lowry, RS Pickart, R Schlitzer. (2017) Late spring nitrate distributions beneath the ice-covered northeastern Chukchi Shelf. J Geophys Res: Biogeosciences 122, 2409-2417, doi:10.1002/2017JG003881.

Brown, ZW, KE Lowry, MA Palmer, GL van Dijken, MM Mills, RS Pickart, KR Arrigo (2015b) Characterizing the subsurface chlorophyll *a* maximum in the Chukchi Sea and Canada Basin. Deep-Sea Res Part II, 118, 88-104.

Buesseler, K, P Boyd (2009) Shedding light on processes that control particle export and flux attenuation in the twilight zone of the open ocean. Limnol Oceanogr 54, 1210–1232.

Cooper, LW, IL Larsen, JM Grebmeier, SB Moran (2005) Rapid deposition of sea ice-rafted material to the Arctic Ocean benthos demonstrated using the cosmogenic tracer ^{7}Be. Deep-Sea Res Part II, 52, 3452–3461.

Falkowski, PG, RT Barber, V Smetacek (1998) Biogeochemical controls and feedbacks on ocean primary production. Science 281, 200-206.

Gardner, WD (2000) Sediment trap sampling in surface waters: issues and recommendations. In: RB Hanson, HW Ducklow, JG Field (Eds.) The changing ocean carbon cycle: a midterm synthesis of the Joint Global Ocean Flux Study. Cambridge University Press, Cambridge, p 240–281.

Gradinger, R (2009) Sea-ice algae: Major contributors to primary production and algal biomass in the Chukchi and Beaufort Seas during May/June 2002. Deep-Sea Res Part II, 56, 1201-1212.

Juul-Pedersen, T, C Michel, M Gosselin (2008) Seasonal changes in the composition and transformation of the sinking particulate material under first-year sea ice in Franklin Bay, Western Canadian Arctic. Mar Ecol Prog Ser 353, 13-25.

Juul-Pedersen, T, C Michel, M Gosselin (2010) Sinking export of particulate organic material from the euphotic zone in the eastern Beaufort Sea. Mar Ecol Prog Ser 410, 55-70.

Knap, A, A Michaels, A Close, H Ducklow, A Dickson (1996) Protocols for the Joint Global Ocean Flux Study (JGOFS) Core Measurements. JGOFS Report Nr. 19, Reprints of Intergovernmental Oceanographic Commission. Manuals and Guides No. 29, UNESCO, Bergen.

Krishnamurthy, D, H Li, F Benoit du Rey, P Cambournac, AG Larson, E Li, M Prakash (2020) Scale-free vertical tracking microscopy. Nature Methods 17, 1040–1051.

Lapoussière, A, C Michel, M Gosselin, M Poulin, J Martin, J-É Tremblay (2013) Primary production and sinking export during fall in the Hudson Bay system, Canada. Cont Shelf Res 52, 62-72.

Pollina T, Larson AG, Lombard F, Li H, Le Guen D, Colin S, de Vargas C and Prakash M (2022) PlanktoScope: Affordable Modular Quantitative Imaging Platform for Citizen Oceanography. Front. Mar. Sci. 9, 949428. doi: 10.3389/fmars.2022.949428

Pommier, J, M Gosselin, C Michel (2009) Size-fractionated phytoplankton production and biomass during the decline of the northwest Atlantic spring diatom bloom. J Plankt Res 31, 429-446.

Sallon, A, C Michel, M Gosselin (2011) Summertime primary production and carbon export in the southeastern Beaufort Sea during the low ice year of 2008. Polar Biol 34, 1989-2005.

Selz, V, S Laney, AE Arnsten, K Lewis, K Lowry, H Joy-Warren, MM Mills, GL van Dijken, KR Arrigo. (2018) Ice algal communities in the Chukchi and Beaufort Seas in spring and early summer: Composition, distributions, and coupling with phytoplankton assemblages. Limnol Oceanogr 63(3), 1109-1133.

Stabeno, PJ, CW Mordy, MF Sigler (2020) Seasonal patterns of near-bottom chlorophyll fluorescence in the eastern Chukchi Sea: 2010–2019. Deep–Sea Res Part II, 177, 104842.